



A Sensitive Yellow Fever Virus Entry Reporter Identifies Valosin-Containing Protein (VCP/p97) as an Essential Host Factor for Flavivirus Uncoating

Harish N. Ramanathan,^a Shuo Zhang,^a Florian Douam,^{b*} Katrina B. Mar,^d Jinhong Chang,^c Priscilla L. Yang,^e John W. Schoggins,^d Alexander Ploss,^b Brett D. Lindenbach^a

^aDepartment of Microbial Pathogenesis, Yale University, New Haven, Connecticut, USA

^bDepartment of Molecular Biology, Princeton University, Princeton, New Jersey, USA

^cDepartment of Experimental Therapeutics, The Baruch S. Blumberg Institute, Doylestown, Pennsylvania, USA

^dDepartment of Microbiology, University of Texas Southwestern Medical Center, Dallas, Texas, USA

^eDepartment of Microbiology and the Blavatnik Institute, Harvard Medical School, Boston, Massachusetts, USA

ABSTRACT While the basic mechanisms of flavivirus entry and fusion are understood, little is known about the postfusion events that precede RNA replication, such as nucleocapsid disassembly. We describe here a sensitive, conditionally replication-defective yellow fever virus (YFV) entry reporter, YFV Δ SK/Nluc, to quantitatively monitor the translation of incoming, virus particle-delivered genomes. We validated that YFV Δ SK/Nluc gene expression can be neutralized by YFV-specific antisera and requires known flavivirus entry pathways and cellular factors, including clathrin- and dynamin-mediated endocytosis, endosomal acidification, YFV E glycoprotein-mediated fusion, and cellular LY6E and RPLP1 expression. The initial round of YFV translation was shown to require cellular ubiquitylation, consistent with recent findings that dengue virus capsid protein must be ubiquitylated in order for nucleocapsid uncoating to occur. Importantly, translation of incoming YFV genomes also required valosin-containing protein (VCP)/p97, a cellular ATPase that unfolds and extracts ubiquitylated client proteins from large complexes. RNA transfection and washout experiments showed that VCP/p97 functions at a postfusion, pretranslation step in YFV entry. Finally, VCP/p97 activity was required by other flaviviruses in mammalian cells and by YFV in mosquito cells. Together, these data support a critical role for VCP/p97 in the disassembly of incoming flavivirus nucleocapsids during a postfusion step in virus entry.

IMPORTANCE Flaviviruses are an important group of RNA viruses that cause significant human disease. The mechanisms by which flavivirus nucleocapsids are disassembled during virus entry remain unclear. Here, we used a yellow fever virus entry reporter, which expresses a sensitive reporter enzyme but does not replicate, to show that nucleocapsid disassembly requires the cellular protein-disaggregating enzyme valosin-containing protein, also known as p97.

KEYWORDS flavivirus, nucleocapsid, uncoating, viral entry

Flaviviruses are a large group of positive-strand RNA viruses classified as a genus, *Flavivirus*, within the family *Flaviviridae*, including several medically important, arthropod-borne human pathogens such as dengue virus (DENV), Japanese encephalitis virus, West Nile virus (WNV), yellow fever virus (YFV), and Zika virus (ZIKV) (1). Infectious virions are small (~50 nm diameter), lipid-enveloped particles that display 180 copies of the envelope (E) glycoprotein and a small transmembrane protein, M, on their surfaces, surrounding an inner nucleocapsid composed of the viral capsid protein

Citation Ramanathan HN, Zhang S, Douam F, Mar KB, Chang J, Yang PL, Schoggins JW, Ploss A, Lindenbach BD. 2020. A sensitive yellow fever virus entry reporter identifies valosin-containing protein (VCP/p97) as an essential host factor for flavivirus uncoating. *mBio* 11:e00467-20. <https://doi.org/10.1128/mBio.00467-20>.

Editor Carolyn B. Coyne, University of Pittsburgh School of Medicine

Copyright © 2020 Ramanathan et al. This is an open-access article distributed under the terms of the [Creative Commons Attribution 4.0 International license](https://creativecommons.org/licenses/by/4.0/).

Address correspondence to Brett D. Lindenbach, brett.lindenbach@yale.edu.

* Present address: Florian Douam, Department of Microbiology, National Emerging Infectious Diseases Laboratories, Boston University School of Medicine, Boston, Massachusetts, USA.

Received 28 February 2020

Accepted 16 March 2020

Published 14 April 2020

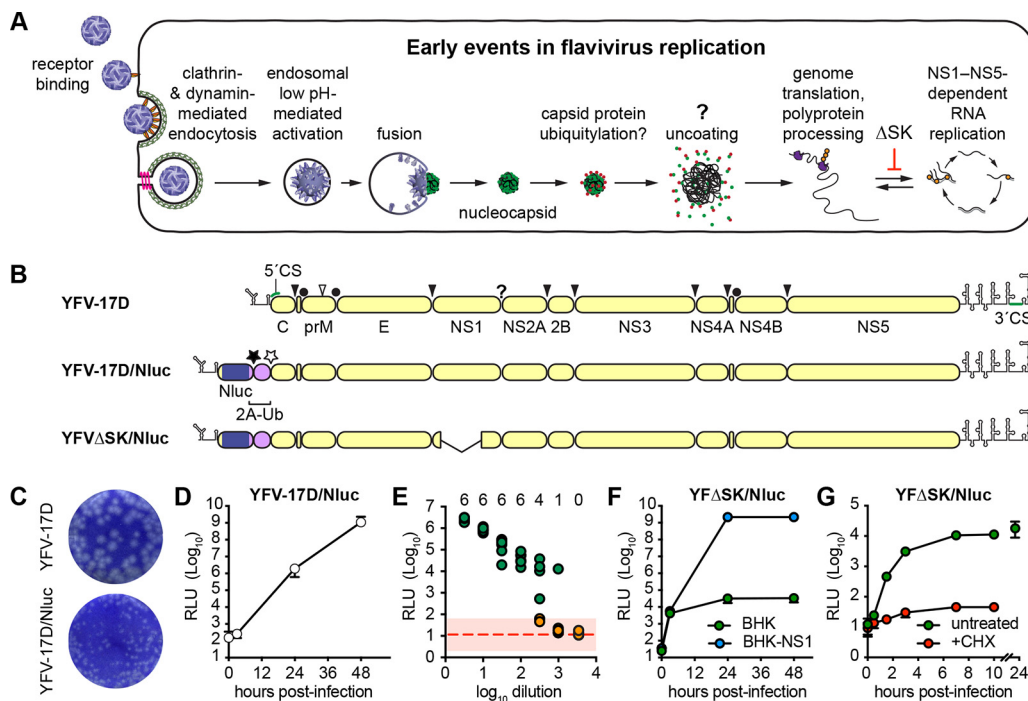


FIG 1 The Nluc reporter virus is a sensitive tool to monitor early events of flavivirus infection. (A) Early steps in the flavivirus life cycle, showing entry, uncoating, translation, and RNA replication. (B) Genome representation and polyprotein processing of YFV-17D, YFV-17D/Nluc, and YFV Δ SK/Nluc reporter viruses used in this study. Circles represent signal peptidase cleavage sites within the YFV polyprotein; filled arrowheads represent YFV NS2B-3 serine protease cleavage sites; the open arrowhead represents a furin cleavage site; the question mark represents cleavage site by an unidentified cellular protease; filled and open stars represent the FMDV 2A translational skipping site and ubiquitin C-terminal hydrolase cleavage site, respectively. (C) Representative wells from YFV-17D and YFV-17D/Nluc plaque assays developed over 5 days with a 0.3% Avicel CL-611 overlay. (D) Time course of Nluc expression after YFV-17D/Nluc infection (MOI of 0.3) of BHK-21 cells. These results are representative of five experiments conducted over different transfection conditions and time scales. (E) Results of a 24-h endpoint dilution assay performed in 6-fold replicate. Wells were scored as positive (green) or negative (orange) based on whether they were $>2\sigma$ (pink rectangle) away from the mean of uninfected controls (dotted red line); the numbers at the top of the graph represent the number of positive wells at each dilution. This experiment was performed three times with similar results. (F) Representative time course of Nluc expression after YFV Δ SK/Nluc infection (MOI of 0.1) of BHK-21 or BHK-NS1 cells. This experiment was performed three times, each with three technical replicates. (G) Representative time course of Nluc expression after YFV Δ SK/Nluc infection (MOI of 0.1) of untreated or CHX-treated BHK-21 cells. This experiment was performed three times, each with three technical replicates. Error bars represent standard deviations from the mean.

and an unsegmented RNA genome of ~ 11 kb (2, 3). While the surface of flavivirus particles is relatively well-defined, nucleocapsid symmetry has been difficult to discern by cryo-electron microscopy (cryo-EM) (2, 4). Recent single-particle cryo-EM analysis and icosahedral averaging suggest that Zika virus nucleocapsid is composed of 20 trimers of dimeric capsid protein, loosely held together under the envelope by lateral interactions involving the capsid $\alpha 5$ helix (5). This is surprising, since $\alpha 5$ serves as a signal peptide for translocation of prM into the endoplasmic reticulum (ER) and must be proteolytically removed by the viral NS2B-3 serine protease in order for prM signal peptidase cleavage to occur, which is required for virus assembly (6–8). These results suggest that additional capsid protein dimers lacking $\alpha 5$ helix may be buried within the RNA core.

Flavivirus infection initiates through interaction of the viral E glycoprotein with one or more host cell attachment factors that serve to concentrate the virions on cell surface, as well as virus entry receptors that have only been partially identified (9). Virus internalization occurs through clathrin- and dynamin-dependent receptor-mediated endocytosis (10). As internalized virus particles pass through endosomes they encounter low pH, which triggers rearrangement of the E glycoprotein, leading to fusion and release of viral nucleocapsids into the cytoplasm of infected cells (Fig. 1A).

Once in the cytoplasm, flavivirus nucleocapsids are presumably disassembled to

release the viral genome, which must be translated in order to initiate replication. The viral genome encodes a single open reading frame, which is translated to produce a polyprotein that is processed by viral and cellular proteases to yield three structural proteins—capsid (C), pre-M (prM), and E—as well as seven nonstructural (NS) proteins: NS1, NS2A, NS2B, NS3, NS4A, NS4B, and NS5 (Fig. 1B). NS1 is a secreted glycoprotein that is required for RNA replication; it forms dimers that remain peripherally associated with the inner leaflet of the ER membrane or on the cell surface, as well as secreted hexameric lipoprotein particles that induce strong humoral responses and contribute to flavivirus pathogenesis (3, 11). NS2A, NS2B, NS4A, and NS4B are polytopic membrane proteins required for RNA replication. NS2B and NS3 form a membrane-anchored enzyme complex with serine protease and RNA helicase activities essential for viral polyprotein processing and RNA replication (3, 12). NS5 is the viral RNA-dependent RNA polymerase and RNA capping enzyme (3, 13, 14). Once translated, the NS proteins presumably recruit the viral genome out of translation and into an RNA replication complex.

Little is known about the process of flavivirus nucleocapsid disassembly. Nucleocapsids obtained by solubilizing WNV particles with nonionic detergent are partially accessible for translation (i.e., a subset of viral proteins can be translated in *in vitro* translation reactions), suggesting that nucleocapsids may spontaneously uncoat (15). On the other hand, intact nucleocapsids can be isolated from detergent-solubilized tick-borne encephalitis virus particles (16); these nucleocapsids dissociate in high salt (0.5 M sodium chloride). In cell culture, however, DENV capsid protein must be ubiquitinated in order for nucleocapsid uncoating and genome translation to occur (17), suggesting that uncoating is an active process *in vivo*.

Here, we describe a sensitive, conditionally replication-defective YFV reporter virus designed to probe the early events of the flavivirus life cycle. We validate the specificity of this reporter to monitor YFV entry and prereplication events, confirm that YFV entry requires ubiquitylation, and then used this tool to examine the hypothesis that YFV nucleocapsids are disassembled by valosin-containing protein (VCP), also known as p97.

VCP/p97 is a conserved and abundant eukaryotic AAA⁺ ATPase that uses the energy released by ATP hydrolysis to unfold ubiquitylated proteins and extract them from large macromolecular complexes (18, 19). VCP/p97 forms hexameric double-ring structures with a central pore (20, 21); each subunit contains an N-terminal regulatory domain and two RecA-like ATPase domains. VCP/p97 plays an essential role in protein homeostasis and genome stability. It is therefore an attractive target for anticancer therapies and several potent and specific VCP/p97 inhibitors have been developed (22). We show here that VCP/p97 is required for a postfusion, prereplication event during YFV entry.

RESULTS

YFV reporter viruses are sensitive tools to monitor early events of flavivirus infection. A key challenge to studying the early life cycle events of flaviviruses is in detecting the translation of incoming, virion-released genomes. While viruses can be engineered to express sensitive reporter genes, signals produced by translation of the incoming viral genome are soon overwhelmed by translation of genomes produced by RNA replication. Therefore, in order to specifically study early, prereplication events in the life cycle of flaviviruses, we sought to uncouple translation from RNA replication by constructing a YFV strain 17D (YFV-17D) reporter that is conditionally defective for RNA replication. The YFV-17D mutant YFV Δ SK, which contains a large, in-frame deletion within the essential NS1 gene, is incapable of initiating RNA replication but can be complemented *in trans* (23). Thus, in the absence of NS1, a YFV Δ SK-based reporter virus should allow viral entry, fusion, uncoating, and primary translation of the incoming genome to be monitored (Fig. 1A).

First, we constructed a full-length, infectious YFV-17D reporter virus that expresses the nanoluciferase (Nluc) enzyme, based on previously described flavivirus reporter

designs (24–26). We chose Nluc because of its smaller size (19.1 kDa; 171 codons), enhanced stability, and exquisite sensitivity compared to other luciferases (27). A cassette encoding Nluc, the foot-and-mouth disease virus 2A translational-skipping peptide (NFDLLKLAGDVESNPG–P; where “–” signifies the unformed peptide bond), and a ubiquitin monomer (MQIFV...LRGG); where “|” signifies cleavage by a ubiquitin C-terminal hydrolase) was inserted in frame into the YFV-17D infectious clone after the first 25 codons of the YFV-17D C gene, which contains the essential 5′ RNA cyclization sequence (28, 29), followed by the entire YFV polyprotein coding sequence, to generate YFV17D/Nluc (Fig. 1B). After transfection into BHK-21 cells, YFV-17D/Nluc RNA transcripts replicated and gave rise to infectious virus with peak titers similar to wild-type YFV-17D ($\geq 1 \times 10^7$ PFU/ml at 48 h posttransfection) but had a small plaque phenotype (Fig. 1C). Similar replication impairments have been reported with other flavivirus reporter constructs (26). Nluc expression was stably maintained for at least three serial virus passages in BHK-21 cells; we did not specifically address the long-term stability of the Nluc insert. Based on prior reports of flavivirus insert instability, we expect that Nluc expression will be lost with passage and therefore limited our experiments to early passage virus stocks. Importantly, YFV-17D/Nluc was able to infect and replicate in BHK cells, as observed by the robust accumulation of Nluc activity over time (Fig. 1D). Robust Nluc expression was also observed upon YFV-17D/Nluc infection of other established cell lines, including HEK 293, HeLa, Huh-7.5, SW-13, and primary mouse fibroblasts (data not shown). Furthermore, Nluc expression levels directly correlated with the amount of input virus in an endpoint dilution assay (Fig. 1E); notably, some replicates became Nluc-negative at higher dilutions, indicating that an endpoint had been reached (i.e., some replicate wells received no virus, while other wells received one or a few viruses). Nluc activity was 10- to 100-fold higher in positive wells around the endpoint, which likely received only a single virus particle, than negative wells (Fig. 1E). Based on this, we were able to calculate a 50% tissue culture infectious dose (TCID₅₀) of 3.54×10^4 TCID₅₀/ml, which was similar to the plaque infectivity titers (3.25×10^4 PFU/ml) of this same early-harvest (18 h posttransfection), low-titer stock. We consistently noted that virus stocks harvested after cytopathic effects became evident contained significant Nluc activity, presumably due to enzyme release into the conditioned medium by cell lysis. Thus, early virus harvests provided optimal signal/noise ratio without requiring extensive washing during virus inoculation (see Materials and Methods for detailed information). Taken together, these data show that YFV-17D/Nluc is a sensitive reporter virus for measuring YFV-17D replication and gene expression at both early and late times postinfection.

Next, we generated a conditionally replication-defective construct, YFV Δ SK/Nluc (Fig. 1B), containing a large in-frame deletion within the essential NS1 gene (23). Upon transfection of RNA transcripts into BHK-21 cells that express YFV NS1 (BHK-NS1), YFV Δ SK/Nluc replicated, expressed Nluc, and produced infectious virus. YFV Δ SK/Nluc virus infected BHK-NS1 cells and expressed robust Nluc activity (Fig. 1F, blue circles); however, infection of parental BHK-21 cells, which do not express NS1, led to modest but significant levels of Nluc expression (Fig. 1F, green circles). To confirm that the Nluc activity observed in BHK-21 cells that lack NS1 expression was due to the entry and translation of YFV Δ SK/Nluc, we performed an additional time course in the presence or absence of cycloheximide (CHX), a potent inhibitor of translation. Nluc expression was detectable as early as 30 min postinfection, increased >10-fold higher than in CHX-treated cells by 90 min postinfection, plateaued by 7 h postinfection, and that Nluc activity persisted for 24 h postinfection (Fig. 1G). Given the tight requirement for NS1 in flavivirus RNA replication, these results demonstrate that YFV Δ SK/Nluc is a sensitive reporter to measure the translation of incoming viral genomes at early times postinfection.

Nluc reporter viruses mimic authentic flavivirus infection and Nluc activity correlates with cellular entry. To further validate the utility of YFV Δ SK/Nluc for monitoring early stages of virus infection, we sought to determine whether it exhibited known features of flavivirus entry and replication. First, we sought to determine

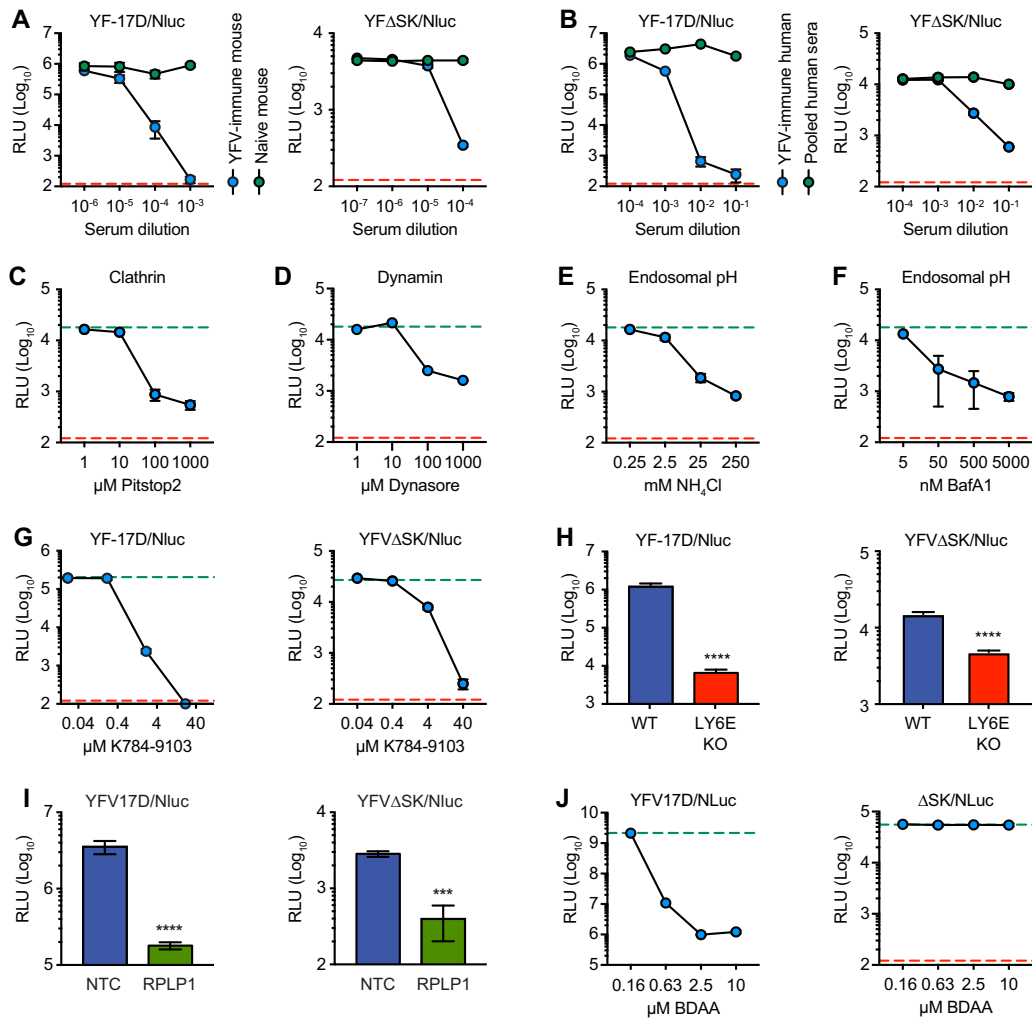


FIG 2 Nluc reporter viruses recapitulate authentic flavivirus infection. (A) Nluc expression after 24 h infection with YFV-17D/Nluc (MOI of 0.3; left panel) or YFVΔSK/Nluc (MOI of 0.1; right panel) pretreated with YFV-immune or control mouse sera in BHK cells. (B) Nluc expression after 24 h infection with YFV-17D/Nluc (MOI of 0.3; left panel) or YFVΔSK/Nluc (MOI of 0.1; right panel) pretreated with YFV-immune or pooled control human sera. (C) Nluc expression at 5 h postinfection with YFVΔSK/Nluc (MOI of 0.1) in cells treated with Pistop2, a potent and specific inhibitor of clathrin-mediated endocytosis. (D) Nluc expression at 5 h postinfection with YFVΔSK/Nluc (MOI of 0.1) of cells treated with Dynasore, a potent and specific inhibitor of dynamin. (E) Nluc expression from YFVΔSK/Nluc infection (MOI of 0.1) of cells treated with NH₄Cl, which buffers the endosomal compartment. (F) Nluc expression at 5 h postinfection with YFVΔSK/Nluc (MOI of 0.1) of cells treated with Bafilomycin A, an inhibitor of endosomal acidification. (G) Nluc expression after 24 h infection with YFVΔSK/Nluc (MOI of 0.1) treated with K784-9103, a potent and specific inhibitor of flavivirus fusion. (H) Nluc expression after infection of wild-type (WT) U2OS or LY6E knockout (KO) U2OS cells with YFV/Nluc (MOI of 0.1) for 24 h (left panel) or YFVΔSK/Nluc (MOI of 0.1) for 6 h (right panel). (I) Nluc expression in HeLa cells transfected with nontargeting control (NTC) or RPLP1-specific siRNAs for 24 h and then infected with YFV/Nluc (MOI of 0.1) for 24 h (left panel) or YFVΔSK/Nluc (MOI of 0.1) for 6 h (right panel). This experiment was repeated twice, each in quadruplicate. (J) Nluc expression after 24 h infection with YFV-17D/Nluc (MOI of 0.3; left panel) or YFVΔSK/Nluc (MOI of 0.1; right panel) in cells treated with BDAA, a potent and specific inhibitor of YFV RNA replication. In all experiments, carrier control treatments are indicated by green dotted lines and the limit of Nluc detection (in parallel CHX-treated cells) by red dotted lines. All data are representative of experiments performed three times, in triplicate except for panel H, which was performed in quadruplicate. Error bars represent standard deviations from the mean. Statistical significance was calculated by using one-way analysis of variance (ANOVA; ****, $P < 0.0001$; ***, $P < 0.001$).

whether Nluc expression was sensitive to YFV-specific neutralizing antibodies. As shown in Fig. 2A, Nluc expression from both YFV-17D/Nluc and YFVΔSK/Nluc was neutralized by serum from an IFNAR1^{-/-} mouse immunized with YFV-17D, while nonimmune control serum did not neutralize Nluc expression. Similarly, serum from a human YFV-17D vaccinee neutralized both reporter viruses, while pooled human serum did not (Fig. 2B). Together, these data confirm that Nluc expression is dependent on infectivity of the YFV reporter viruses.

Flaviviruses enter target cells via receptor-mediated endocytosis, which requires clathrin and dynamin, and delivery to endosomes, where viral fusion is induced by the low pH of this compartment (30). Consistent with this viral entry pathway, expression of Nluc by YFV Δ SK/Nluc was sensitive to Pitstop2, an inhibitor of clathrin-coated pit formation (Fig. 2C), and to Dynasore, an inhibitor of dynamin (Fig. 2D). Furthermore, expression of Nluc by YFV Δ SK/Nluc was sensitive to ammonium chloride (NH₄Cl), a weak base that buffers endolysosomal compartments (Fig. 2E), and to bafilomycin A1 (BafA1), an inhibitor of the vacuolar H⁺-ATPase pump (Fig. 2F). As shown in Fig. 2G, YFV-mediated Nluc expression was sensitive to K784-9103, a small-molecule that binds to DENV E protein and inhibits membrane fusion of DENV and other flaviviruses (31). Furthermore, YFV-mediated Nluc expression was reduced by genetic ablation of LY6E (Fig. 2H), a host factor that facilitates internalization of flaviviruses and other viruses (32, 33), or by RNAi-mediated knockdown of RPLP1 (Fig. 2I), a ribosomal protein required for efficient flavivirus translation (34). These results confirm that YFV/Nluc and YFV Δ SK/Nluc gene expression are dependent on clathrin, dynamin, LY6E-mediated trafficking, endosomal acidification, and YFV E-mediated fusion, consistent with the known pathways of flavivirus entry.

We also examined the effects of benzodiazepine acetic acid (BDAA), a low-molecular inhibitor of YFV RNA replication that targets NS4B (35). In contrast to the entry-specific inhibitors used above, BDAA potently inhibited Nluc expression by YFV-17D/Nluc but had no effect on Nluc expression by YFV Δ SK/Nluc (Fig. 2J), confirming that YFV Δ SK/Nluc is a sensitive reporter of prereplication events in the YFV life cycle.

Ubiquitylation and valosin-containing protein (VCP/p97) are essential for early stages of YFV infection. Since DENV genome uncoating requires ubiquitylation, presumably of the incoming capsid protein (17), we next examined whether early YFV gene expression also requires ubiquitylation. As shown in Fig. 3A, expression of Nluc activity during YFV Δ SK/Nluc infection was blocked by Pyr-41, a potent, specific, and irreversible inhibitor of the ubiquitin-activating enzyme E1 (36), confirming that ubiquitylation is required for an early, prereplication event in the YFV life cycle. To clarify the stage in entry where ubiquitylation is required, we bypassed the viral entry process by directly transfecting YFV Δ SK/Nluc RNA into BHK cells. As shown in Fig. 3B, Pyr-41 did not inhibit Nluc expression after RNA transfection. These results show that ubiquitylation is required for an early step in YFV entry, upstream of genome release (i.e., uncoating), consistent with the finding that ubiquitylation is required for the disassembly of the DENV nucleocapsid (17).

These results suggested that ubiquitin can tag incoming nucleocapsids for subsequent uncoating by an unidentified host factor. The eukaryotic AAA⁺ ATPase VCP/p97 utilizes energy released from ATP hydrolysis to unfold ubiquitylated client proteins and extract them from larger complexes (18). We therefore tested the hypothesis that VCP/p97 promotes disassembly of the YFV nucleocapsid. As VCP/p97 is an abundant cellular protein, efficient knockdown takes several days to achieve a loss-of-function phenotype, which can cause pleiotropic effects on cells (37). Therefore, in order to specifically examine the role of VCP/p97 in YFV entry we chose two small molecules, DBEQ (an ATP competitor) and NMS-873 (an allosteric inhibitor), which work through different mechanisms of action to potentially and specifically inhibit VCP/p97 in a matter of minutes, rather than days (38, 39). DBEQ and NMS-873 potently inhibited Nluc expression after infection with YFV Δ SK/Nluc virus particles (Fig. 3A) but did not inhibit Nluc expression after transfection of YFV Δ SK/Nluc RNA (Fig. 3B), indicating that VCP/p97 is necessary for YFV entry, prior to the delivery and translation of incoming YFV genomes.

To clarify the step at which VCP/p97 functions during YFV entry, we conducted a washout experiment. As shown in Fig. 3C, DBEQ inhibition of YFV Δ SK/Nluc entry could be reversed by drug washout at 1 h postinfection. Moreover, DBEQ washout bypassed the sensitivity to BafA1, indicating that VCP/p97 functions at a postfusion step of YFV entry. We were unable to perform the converse experiment, washout of BafA1, followed by DBEQ treatment, because BafA1 washout was highly inefficient, consistent with the

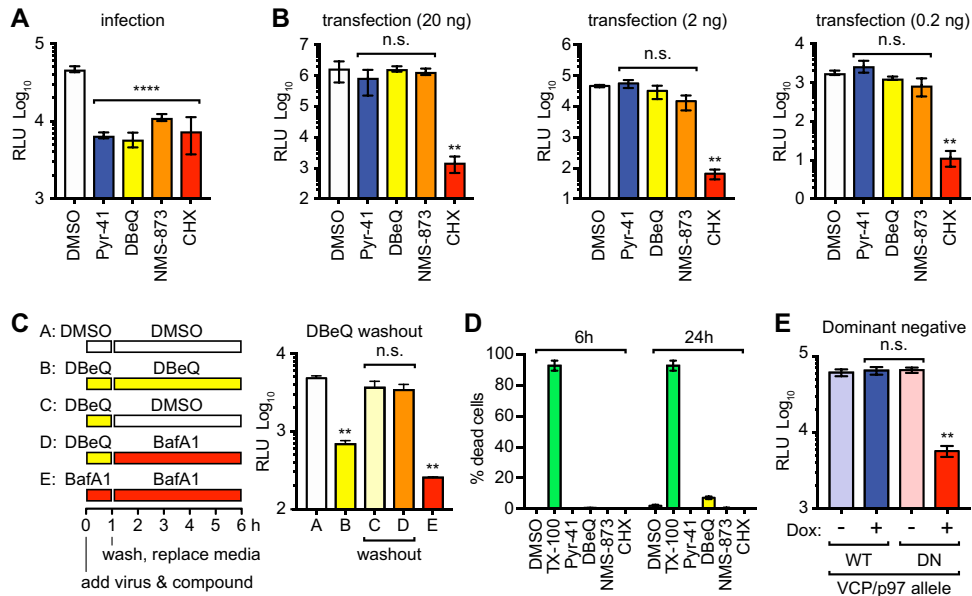


FIG 3 VCP/p97 is essential for an early, postfusion stage of YFV Δ SK/Nluc virus infection. (A) Nluc expression at 5 h postinfection with YFV Δ SK/Nluc (MOI of 0.1) of BHK cells treated with Pyr-41 (50 μ M), DBeQ (10 μ M), NMS-873 (300 nM), or CHX (100 μ g/ml). This experiment was performed in triplicate and is representative of five independent experiments; error bars represent SD from the mean. (B) Nluc expression at 5 h posttransfection with 20 ng (left panel), 2 ng (middle panel), or 0.2 ng (right panel) YFV Δ SK/Nluc RNA in BHK cells treated with the indicated compounds, as described above. This entire experiment was performed twice. (C) Nluc expression at 6 h postinfection with YFV Δ SK/Nluc (MOI of 0.1) in BHK cells continuously treated with DMSO carrier control, DBeQ, or BafA1, as well as cells treated with DMSO or DBeQ and subjected to washout conditions, as indicated in the left panel and detailed in Materials and Methods. This experiment was performed three times, each in triplicate, with similar results. (D) Drug toxicity was quantified by plotting the percentage of dead cells against various inhibitor or control treatments, as above, at the indicated time points. Statistical significance was calculated by using ordinary one-way ANOVA (****, $P < 0.0001$; ***, $P < 0.001$; **, $P < 0.01$; *, $P < 0.05$; ns, not significant). This experiment was repeated twice with similar results. (E) Nluc expression at 6 h postinfection of Flp-In T-Rex-293 cells induced to express a WT or dominant negative (DN) allele of VCP/p97 for 24 h prior to infection. This experiment is representative of three independent experiments, each performed in triplicate.

low nanomolar dissociation constant of this compound (40). Importantly, Pyr-41, DBeQ, NMS-873, and CHX treatments were not toxic under the concentrations and time scales used in our studies (Fig. 3D), indicating that their abilities to block viral gene expression were not simply due to cellular toxicity. Moreover, the expression of a dominant negative allele confirmed that VCP/p97 is required for early YFV gene expression (Fig. 3E). Taken together, these data suggest that VCP/p97 functions at a postfusion, prereplication step in the YFV life cycle.

VCP/p97 is required for early events in the flavivirus life cycle. To determine whether ubiquitylation and VCP/p97 are also required for postreplication viral gene expression, we examined Nluc expression by the replication-competent YFV-17D/Nluc. As shown in Fig. 4A and B, Pyr-41 and DBeQ potently inhibited Nluc expression by 18 h postinfection with YFV-17D/Nluc, but not after 18 h posttransfection of YFV-17D/Nluc RNA. Since robust expression of Nluc activity at late times of infection (>8 h) depends on YFV-17D/Nluc replication (compare Fig. 1D, F, and G), these data suggest that ubiquitylation and VCP/p97 are specifically required for early events in the YFV life cycle.

We next examined whether other flaviviruses depend on ubiquitylation and VCP/p97 activity. As shown in Fig. 4C, Pyr-41, DBeQ, and CHX all potently inhibited detectable expression of NS1 by 24 h postinfection with the Kunjin strain of WNV (WNV_{KUN}) or Cambodian FSS 13025 strain of ZIKV. These data suggest that multiple flaviviruses depend on cellular ubiquitylation and VCP/p97 activity.

Finally, we examined whether VCP/p97 activity was also required for early YFV gene expression in mosquito cells. Sequence alignment showed that the *Aedes albopictus*

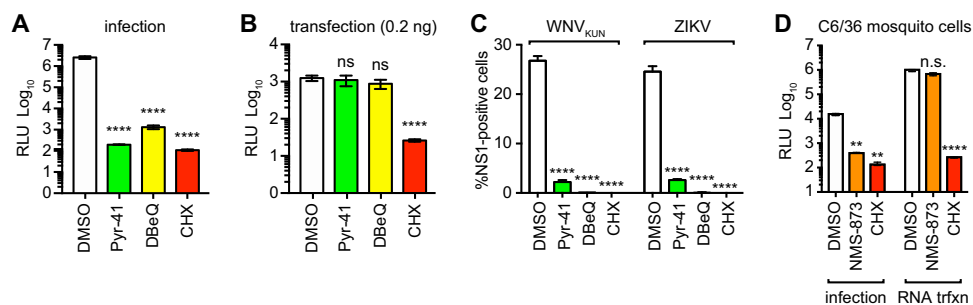


FIG 4 VCP/p97 activity is required for flavivirus infection. (A) Nluc expression at 18 h postinfection with YFV-17D/Nluc (MOI of 0.3) of cells treated with the indicated compounds: Pyr-41 (50 μ M), DBeQ (10 μ M), NMS-873 (300 nM), or CHX (100 μ g/ml). (B) Nluc expression at 5 h posttransfection with 0.2 ng YFV-17D/Nluc RNA in cells treated with the indicated compounds, as described above. (C) Infection of BHK cells with WNV_{KUN} or ZIKV (each at an MOI of 1.0) in cells treated with the indicated compound, as described above. Cells were fixed at 24 h postinfection, stained for NS1 expression, and counted by flow cytometry, as detailed in Materials and Methods. (D) Nluc expression at 6 h after pretreating C6/36 mosquito cells for 1 h with the indicated compounds, followed by infection with YFV Δ SK/Nluc (MOI of 0.3) or transfection with 20 ng of YFV Δ SK/Nluc RNA (as indicated). The experiments depicted in panels A and D were performed three times, each in triplicate. The experiments depicted in panels B and C were performed twice in parallel, each in triplicate. Statistical significance was calculated by using one-way ANOVA (****, $P < 0.0001$; ***, $P < 0.001$; **, $P < 0.01$; *, $P < 0.05$; ns, not significant).

and *Aedes aegypti* TER94 genes share 99.75% identity to one another and 84.89% identity to human VCP/p97 (see Fig. S1A to C in the supplemental material), including conserved ATPase active-site residues and residues involved in binding to allosteric inhibitors (39). Consistent with these observations, we found that NMS-873 inhibited YFV Δ SK/Nluc gene expression in C6/36 *Aedes albopictus* cells; however, this inhibition was bypassed by transfecting YFV Δ SK/Nluc RNA into these cells (Fig. 4D). These data suggest that the mosquito homolog of VCP/p97, TER94, also functions at an early step in flavivirus entry.

DISCUSSION

The processes of flavivirus internalization and fusion were originally characterized by using biochemical and cell biological approaches with high MOIs of radiolabeled virus particles, revealing a requirement for endocytosis and endosomal acidification (41, 42). While working with infectious, radiolabeled virus particles may be inconvenient, the use of high MOIs is potentially more problematic, since aggregates of virus particles can influence the apparent mechanisms of viral entry (43). More recently, the entry of individual, fluorescently labeled flavivirus particles has been visualized at low MOIs through live cell imaging (30, 44–46). An important caveat to this approach is that flavivirus preparations typically have relatively low specific infectivities (44, 45, 47), so it is difficult to know whether a given particle under observation is on a pathway toward productive infection.

Given these considerations, we chose to pursue a function-based approach to study the productive entry of a recombinant YFV that expresses a reporter enzyme only after viral entry and translation. Several flavivirus reporter systems have been developed, mainly for high-throughput screening of viral replication (17, 26, 48–55). In one remarkable study, Byk et al. adapted a *Renilla* luciferase-expressing DENV reporter virus to show that the incoming DENV capsid protein must be ubiquitinated prior to viral gene expression (17). However, an important consideration of this experimental design is that flavivirus-encoded reporter genes are continuously expressed, making it difficult to rigorously conclude that reporter activity was translated from an incoming viral genome versus viral RNAs produced by replication, i.e., because both viral entry and RNA replication can contribute to reporter gene expression, the translation of incoming genomes could only be inferred based on the kinetics of when reporter gene expression first became observable. Byk et al. attempted to control for this concern by using CHX to inhibit translation (17); however, CHX inhibits viral gene expression irrespective of whether the genome was delivered by a virus particle or newly synthesized by RNA

replication. A further consideration is that reporter enzymes differ in their specific activities; thus, enzymes with low specific activity require higher MOIs to achieve similar sensitivity of early translation events. In this regard, it is notable that Byk et al. did not report the MOIs used in their DENV entry studies; however, several of their experiments used MOIs sufficiently high to allow incoming capsid protein to be detected by Western blotting (17). Despite these minor technical caveats, Byk et al. clearly demonstrated that incoming DENV capsid protein is degraded in a ubiquitin-dependent process and that ubiquitylation is needed before viral gene expression can be detected.

Given these considerations, we sought to build a sensitive YFV reporter specific for detecting translation of incoming viral genomes. First, we used the Nluc reporter gene, which exhibits >100-fold greater specific activity over firefly and *Renilla* luciferases (56). Second, we created a conditionally replication-defective reporter by incorporating a large, in-frame deletion in the essential NS1 gene, which can be supplied in *trans* (23, 57). The NS1 glycoprotein, which is expressed within the secretory pathway, contributes to the cytosolic process of RNA replication via interaction with the polytopic NS4A and NS4B membrane proteins, likely within the NS4A-2K-NS4B polyprotein intermediate (58–60). NS1 also has distinct membrane alteration properties (59, 61), which likely contribute to replication complex assembly. In the absence of NS1 expression, flavivirus infections are halted prior to replication complex formation and the initial round of RNA synthesis (23, 59, 62, 63). Consistent with this, robust Nluc expression by YFV-17D/Nluc was sensitive to a YFV-specific RNA replication inhibitor, BDAA, while the modest Nluc expression by YFVΔSK/Nluc was not. Thus, the YFVΔSK/Nluc virus faithfully reports on early, postfusion, prereplication events in the flavivirus life cycle.

Our experimental approach should be generally applicable to other flaviviruses. It is notable that two groups previously described NS1 deletion reporter virus systems for WNV and Omsk hemorrhagic fever virus (55, 64). These constructs were originally designed to reduce biosafety risks for high-throughput screening; our data suggest that these constructs should also be useful in dissecting early, prereplication events in the life cycle of these flaviviruses. Further improvements to our design are also possible; for instance, smaller tags, such as a split Nluc reporter (53), could improve viral titers or allow postfusion events to be monitored prior to viral genome translation.

We validated that YFVΔSK/Nluc gene expression was neutralized by YFV-specific antibodies and was dependent on several known pathways of flavivirus entry, including clathrin- and dynamin-mediated endocytosis (10, 30, 65–67), endosomal acidification (45, 66–69), E protein-dependent fusion (31), and dependence on LY6E (32, 33) and RPLP1 (34).

We then applied our YFV reporter system to address the role of ubiquitylation and protein homeostasis in flavivirus entry, which has been controversial. As part of a genome-wide RNAi screen, Krishnan et al. first reported that knockdown of ubiquitin ligase CBLL1 inhibited internalization of WNV particles into HeLa cells and that WNV entry was sensitive to proteasome inhibitors (70). However, these findings were called into question by Fernandez-Garcia et al., who found that the entry of WNV, YFV, and DENV was insensitive to rigorously validated knockdown of CBLL1 or by proteasome inhibitors (71). Furthermore, while JEV entry is also inhibited by proteasome inhibitors (72), these compounds can decrease the cellular pools of free ubiquitin (73–75), so the role of ubiquitylation versus proteasome activity in flavivirus entry has been unclear. Byk et al. brought clarity to this issue by demonstrating that ubiquitylation is required for DENV capsid disassembly (17). Furthermore, proteasome activity is dispensable for DENV entry but is responsible for the turnover of incoming capsid protein, presumably after disassembly (17).

Our studies confirm that ubiquitylation is required for flavivirus entry, although the relevant substrate(s) are unknown. Given that incoming DENV capsid protein is turned over in a proteasome-dependent manner and that inhibition of proteasome activity leads to the accumulation of a slightly higher molecular weight form of capsid protein (17), it is likely that flavivirus capsid proteins are directly ubiquitylated. It is not yet clear how nucleocapsids are targeted for ubiquitylation, nor whether there is a preferred site

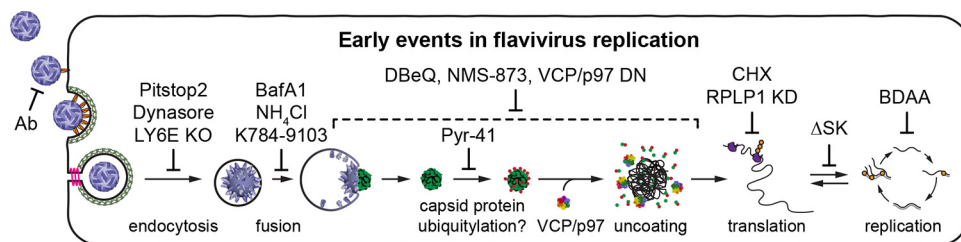


FIG 5 Revised model for the early, prereplication events in flavivirus infection (modified from Fig. 1A). After fusion, the nucleocapsid is exposed to the cytosol, where capsid protein (green circles) is presumably ubiquitinated (red hexagons), leading to VCP/p97-dependent nucleocapsid disassembly and release of the viral genome prior to translation. Inhibitors used in this study are indicated. The dotted line indicates the range where VCP/p97 functions in flavivirus entry.

on capsid protein for this modification. In this regard, DENV mutants lacking lysine residues in the capsid protein were able to infect and translate their genomes normally (17), suggesting that the capsid protein may be ubiquitylated at the N terminus or other noncanonical residue(s) (76). Future work would be needed to identify of the relevant E3 ligase(s) and the type(s) of ubiquitin linkage that modify flavivirus capsid proteins.

VCP/p97 functions to unfold and extract proteins from macromolecular complexes in a ubiquitin- and ATP-dependent manner (18). For instance, VCP/p97 dissociates ubiquitylated $\text{I}\kappa\text{B}\alpha$ from NF- κB , activating this transcription factor (77). VCP/p97 contributes to ER-associated degradation by extruding misfolded proteins from the secretory pathway for subsequent delivery to the proteasome (78). Similarly, VCP/p97 contributes to ribosome-associated quality control by extracting misfolded nascent polypeptides from the translation apparatus (79, 80). VCP/p97 has additional roles in extracting client substrates from chromatin, mitochondria, and other large macromolecular complexes. It is worth noting that VCP/p97 has a weak affinity for ubiquitin and relies on a large array of cofactors, which typically encode enzymatic activities to facilitate VCP/p97 substrate processing, or adaptor molecules, which simply link VCP/p97 to client substrates. Each of these adaptors and cofactors carry binding surfaces that recognize VCP/p97 and ubiquitin, respectively (81, 82). Thus, VCP/p97 contributes to diverse cellular functions based this modular cofactor- and adaptor-mediated targeting strategy.

Based on our finding that VCP/p97 activity is required for an early, postfusion event prior to the translation and replication of incoming YFV genomes, we propose a model wherein VCP/p97 functions to disassemble ubiquitylated nucleocapsids (Fig. 5). As mentioned above, direct evidence for ubiquitylation of incoming flavivirus capsid protein is currently lacking, although capsid is degraded by the proteasome in a ubiquitin-dependent manner. Although we have illustrated free nucleocapsids within the cytosol, we cannot exclude the possibility that fusion is tightly coupled to capsid ubiquitylation and disassembly, such that nucleocapsids may be ubiquitylated and disassembled as they are exposed to the cytosol. Consistent with our model, VCP/p97 activity was previously shown to be important for WNV, JEV, and DENV infection, although specific role(s) for VCP/p97 in virus entry were not determined (53, 83). Similarly, VCP/p97 is also important for an early step, upstream of N-protein degradation, during the entry of infectious bronchitis virus, a coronavirus (84). VCP/p97 also contributes to productive trafficking of NRAMP2, a cellular receptor for the entry of Sindbis virus, an alphavirus (85). Thus, VCP/p97 appears to play a general role in the entry of enveloped RNA viruses and may also contribute to RNA replication of alphaviruses (86) and hepaciviruses (87, 88). Given these findings, it will be interesting to determine whether VCP/p97 inhibitors have therapeutic potential in viral infections.

MATERIALS AND METHODS

Cell lines and plasmids. Baby hamster kidney (BHK-21), clone 15 cells, BHK-21 cells stably expressing YFV-NS1 (BHK-NS1), HeLa cells, WT U2OS cells, and LY6E-knockout U2OS cells were maintained in Dulbecco minimal essential medium (DMEM; Life Technologies, Inc., Gaithersburg, MD) supplemented

with 10% heat-inactivated fetal bovine serum (FBS; Omega Scientific) and 1 mM nonessential amino acids (here referred to as complete medium) at 37°C and 5% CO₂. Flp-In T-Rex-293 cells were purchased from Invitrogen and maintained at 37°C and 5% CO₂ in complete medium containing 100 µg/ml zeocin and 15 µg/ml blasticidin. C6/36 cells were maintained at 30°C and 5% CO₂ in MEM containing 10% FBS and 1 mM nonessential amino acids.

The construction and maintenance of pCC1/YF17D and pYF-17D/5'C25Venus2Aubi have been described (24, 25). Plasmid pYF17D/Nluc was constructed by replacing the Venus coding region of pYF-17D/5'C25Venus2Aubi with that of the Nluc gene (Promega, Madison, WI) by using standard molecular biology techniques and verified by restriction digestion and sequencing. Briefly, the SrfI-Nsil region of pYF17D/5'C25Venus2Aubi was subcloned into a shuttle vector, pSL1180, generating the pSL1180/S17DN intermediate. The Nluc coding region was PCR amplified with the primers YO-3008 (5'-ggg ccc GAG CTC ATG GTC TTC ACA CTC GAA GAT TTC GTT G-3') and YO-3009 (5'-ggg ccc acc ggt CGC CAG AAT GCG TTC GCA CAG CCG CCA GC-3') and Q5 polymerase (NEB) and then cloned into the SacI and AgeI sites of pSL1180/S17DN, resulting in replacement of Venus with Nluc. The SrfI-Nsil fragment was then subcloned back into pCC1/YF-17D to generate pYF17D/Nluc. The construction and use of pYFΔSK, as well as pSINrep21-NS1, were described previously (23, 62). To generate pYFΔSK/Nluc, the 7221-bp Nsil-ClaI fragment of pACNR/YFΔSK was subcloned into pYFV17D/Nluc cut with these same enzymes.

To generate Flp-In T-Rex-293 cells expressing WT VCP/p97 or a dominant negative mutant (K251Q/K524Q) form of VCP/p97, the VCP/p97 gene was amplified from pcDNA3.1(+)/p97-WT or pcDNA3.1(+)/p97-QQ (89), kindly provided by Christian Schlieker (Yale University), by using the primers YO-3508 (5'-CCA GCC TCC GGA CTC TAG CGT TTA AAC TTA GCC ACC ATG GCT TCT GGA GCC GATT-3') and YO-3509 (5'-TGA TGA TGA CCT GTA TGG CTA AGT ACC GAG CTC GGA TCC ACT AGT CCA GT-3') and cloning the fragment into HindIII-cut pcDNA5/FRT/TO (Invitrogen) by using Gibson assembly (NEB). The resulting vectors were cotransfected into Flp-In T-Rex-293 cells with pOG44 (at a 1:9 mass ratio), and stable cells were selected in complete medium containing 50 µg/ml hygromycin and 15 µg/ml blasticidin. Cells were induced to express VCP/p97 by adding 3 µg/ml doxycycline to complete medium for 24 h.

Transfections and virus stocks. Small scale RNA transfections were performed by using *TransIT* mRNA transfection reagent (Mirus Bio) according to manufacturer's recommendations. BHK-NS1 stable cells were regenerated as previously described (23). Briefly, 1 µg of pSINrep21/YFV NS1 plasmid DNA was transfected into BHK-21 clone 15 cells by using 8 µl of *TransIT* LT1 reagent (Mirus Bio, Wisconsin, MD) and low-serum Opti-MEM (Life Technologies). Transfected cells were then selected for 1 week in complete growth medium supplemented with 5 µg/ml puromycin. Reporter virus RNAs were transcribed from XhoI-linearized plasmid templates pYF17D/Nluc and pYFΔSK/Nluc by using SP6 RNA polymerase in the presence of the ARCA synthetic cap analog (New England Biolabs, Ipswich, MA). Primary stocks of reporter virus were generated by electroporation of BHK-21 clone 15 or BHK-NS1 cells with YFV RNA transcripts, as previously described (23). At 36 h postelectroporation, conditioned media containing primary YFV-17D/Nluc or YFVΔSK/Nluc stocks were harvested and clarified by centrifugation at 3,000 × *g* at 4°C for 10 min to remove cell debris.

Pilot experiments showed that primary stocks of YFV-17D/Nluc virus harvested at late time points (≥36 h posttransfection) contained high levels of Nluc released into the conditioned cell culture media, which correlated with the onset of virus-induced cytopathic effects. Therefore, to help minimize background, primary stocks of Nluc-expressing virus were dialyzed via ultrafiltration with Centricon plus-80 (containing 100-kDa nominal molecular weight cutoff polyethersulfone filters) to remove contaminating background Nluc activity. Furthermore, secondary virus stocks with minimal Nluc background were harvested at early (<24 h) times postinfection, albeit with reduced titers. Specifically, primary virus stocks were passaged on several 15-cm dishes of ~70% confluent monolayers of BHK-21 or BHK-NS1 cells; after 1 h of incubation at 37°C, the inoculum was removed, washed twice with complete DMEM and twice with phosphate-buffered saline (PBS), and then incubated in the presence of complete DMEM containing 2% FBS. Conditioned cell culture media were harvested ~18 h postinoculation, clarified as before, and stored in 1-ml aliquots at -80°C. These early harvest virus stocks had very low contaminating Nluc activity that was effectively removed by washing infected cells three times with PBS.

Virus infectivity. Infectivity measurements were determined by using plaque assays or endpoint dilution assays. Plaque assays were performed as previously described (90). For endpoint dilution assays with Nluc viruses, virus stocks were serially diluted in half-log ($\sqrt{10}$) intervals in DMEM containing 2% FBS and nonessential amino acids; each dilution was then added to BHK cells seeded in 96-well plates. At 24 h postinfection, cells were washed twice with complete DMEM and once with PBS, and the Nluc activity was measured in all wells. Wells were scored positive if the Nluc activity was >2σ from the mean of uninfected controls. Tissue culture infectious dose 50% endpoint (TCID₅₀) values were calculated by using the method of Reed and Muench method, as previously described (58).

Nluc activity. Nluc activity was measured by using the Nano-Glo luciferase assay (Promega). At the indicated times in the assay, cells grown in 96-well plates were gently washed twice with complete DMEM and once with PBS and then lysed with 20 µl of Nano-Glo luciferase assay buffer containing the substrate. The Nluc activity was measured from cell lysates within 10 min of lysis (or substrate addition) by transferring lysate into white OptiPlate 96-well plates (Perkin-Elmer, Waltham, MA) and measured in a Berthold Centro X53 LB 960 luminescent plate reader with readings integrated over 0.2 s.

Inhibitors and treatments. Ammonium chloride, BafA1, cycloheximide, and DBeQ were purchased from Millipore-Sigma (Burlington, MA). Pitstop2 and Dynasore were purchased from Abcam, Cambridge, MA. Pyr-41 was purchased from MedChemExpress (Monmouth Junction, NJ). NMS-873 was purchased

from Tocris (Minneapolis, MN). Except where noted, all drugs were added to cells 1 h prior to infection or RNA transfection at the following concentrations: Pyr-41 (50 μ M), DBeQ (10 μ M), NMS-873 (300 nM), and CHX (100 μ g/ml) and maintained in the cell culture medium throughout the experiments. The DENV fusion inhibitor K784-9103 was purchased from ChemDiv (San Diego, CA), and its structure and purity were confirmed by tandem liquid chromatography-mass spectrometry. Inhibition of E-mediated fusion was performed as previously described (31). Briefly, reporter viruses were incubated in medium containing the indicated concentrations of K784-9103 and then mixed in a rotary shaker for 30 min at room temperature to allow inhibitor to bind to virus particles before adding to cells.

DBeQ washout experiments were performed by adding 0.1% dimethyl sulfoxide (DMSO), 10 μ M DBeQ, or 50 nM BafA1 with YFV Δ SK/Nluc virus (i.e., no preincubation of cells). At 1 h postinfection, all cells were washed twice with complete medium and twice with PBS and then returned to media containing 0.1% (vol/vol) DMSO, 10 μ M DBeQ, or 50 nM BafA1, as indicated. Samples were collected 6 h later.

RPLP1 was transiently knocked down in HeLa cells by reverse transfection of ON-TARGETplus Human RPLP1 SMARTPool small interfering RNA (siRNA; Dharmacon catalog no. L-011135-00-0005) or AllStars Negative Control siRNA (Qiagen catalog no. 1027280) as a negative control. Briefly, siRNA transfection mixtures were assembled with Lipofectamine RNAiMAX (Invitrogen) and plated in 96-well plates before seeding HeLa cells. After 48 h postseeding, the cells were used for infection experiments.

Virus neutralization assay. C57BL/6J IFNAR^{-/-} mice (91) were kindly provided by Sergei Kotenko, Rutgers University. Mice were bred in the Laboratory Animal Resource Center of Princeton University. All animal experiments were performed in accordance to protocol number 1930, which was reviewed and approved by the Institutional Animal Care and Use Committee (IACUC) of Princeton University. One female, 6-month-old mouse was infected intravenously with 1×10^7 PFU of YFV-17D. At 18 days postinfection, the mouse was boosted intravenously with 1×10^7 PFU of YFV-17D. Serum was collected 7 days after this booster injection. Serum from an uninfected female C57BL/6J IFNAR^{-/-} littermate (6 months old) was collected in parallel for use as a negative control. The YFV-immune human serum was obtained from a deidentified donor through the American Red Cross. Pooled human sera was purchased from Thermo-Fisher (Waltham, MA) for use as a negative control. For virus neutralization experiments, mouse and human sera were diluted into reporter virus stocks, and samples were incubated for 30 min at room temperature with tumbling. At the end of the incubation, samples were centrifuged briefly and 50- μ l samples were added to three wells of BHK cells grown in 96-well plates. The Nluc expression was measured after 5 h of infection.

Cytotoxicity assay. Cells were seeded in 96-well plates and incubated with inhibitors at their respective experimental concentrations (indicated above) along with the membrane-impermeable nuclear dye Cytotox Green (Essen BioScience, Inc. Ann Arbor, MI) and cell-permeable Hoechst stain (Sigma). Cytotoxicity was measured on an ImageXpress Pico (Molecular Devices) by quantifying the fraction of Cytotox Green-positive, permeable cells among total cells.

Immunostaining and FACS analysis. WNV_{KUN} and ZIKV NS1 were detected by immunostaining with 6B8-2D8, a flavivirus NS1 cross-reactive monoclonal antibody, originally raised against DENV-4 NS1 (kindly provided by Marie Flamand, Institut Pasteur). Briefly, cells were washed twice with PBS and treated with Accumax (Innovative Cell Technologies, Inc., San Diego, CA) to gently dissociate cells for fluorescence-activated cell sorting (FACS) analysis. Dissociated cells were directly fixed in paraformaldehyde solution (2% [wt/vol] final) for 30 min at room temperature. Fixed cells were permeabilized with 0.2% saponin for ~30 min on a rotating chamber, followed by two washes with PBS. Cells were incubated overnight with a 1:3,000 dilution of NS1-specific antibody 6B8-2D8 in PBS containing 2% FBS, washed with PBS, and incubated with 1:1500 dilution of an anti-mouse secondary antibody conjugated to Alexa 680 fluorescent dye. The specificity of labeling was confirmed by parallel incubation with the dye-conjugated secondary antibody in the absence of primary antibody and by performing the complete staining procedure on uninfected cells. At the end of incubation, the cells were washed twice, resuspended in PBS, and subjected to FACS analysis to quantify the percentage of NS1-positive cells by using the far-red channel.

SUPPLEMENTAL MATERIAL

Supplemental material is available online only.

FIG S1, PDF file, 0.1 MB.

ACKNOWLEDGMENTS

We thank Charles M. Rice (The Rockefeller University) for providing pACNR/YF17D, pACNR/YFASK, pSINrep21/YF NS1, pCC1/YF17D, and pYF-17D/5'C25Venus2AUBi; Marie Flamand (Institut Pasteur) for providing NS1-specific monoclonal antibodies; Sergei Kotenko (Rutgers University) for providing C57BL/6J IFNAR^{-/-} mice; Doug Brackney (Connecticut Agricultural Experiment Station) for providing BHK-21 clone 15 cells; and Christian Schlieker for providing pcDNA3.1(+)/VCP/p97-WT and pcDNA3.1(+)/VCP/p97-QQ.

This study was supported by PHS grants AI087925, AI131518, and AI120113 (all to B.D.L.) and AI107301 (to A.P.) and by a Burroughs-Wellcome Fund Investigator in Pathogenesis Award (101539) to A.P.

REFERENCES

1. Simmonds P, Becher P, Bukh J, Gould EA, Meyers G, Monath T, Muerhoff S, Pletnev A, Rico-Hesse R, Smith DB, Stapleton JT, Ictv RC. 2017. ICTV virus taxonomy profile: *Flaviviridae*. *J Gen Virol* 98:2–3. <https://doi.org/10.1099/jgv.0.000672>.
2. Kuhn RJ, Zhang W, Rossmann MG, Pletnev SV, Corver J, Lenches E, Jones CT, Mukhopadhyay S, Chipman PR, Strauss EG, Baker TS, Strauss JH. 2002. Structure of dengue virus: implications for flavivirus organization, maturation, and fusion. *Cell* 108:717–725. [https://doi.org/10.1016/s0092-8674\(02\)00660-8](https://doi.org/10.1016/s0092-8674(02)00660-8).
3. Lindenbach BD, Murray CL, Thiel HJ, Rice CM. 2013. *Flaviviridae*, p 712–746. In Knipe DM, Howley PM (ed), *Fields virology*, 6th ed. Lippincott/Williams & Wilkins, Philadelphia, PA.
4. Therkelsen MD, Klose T, Vago F, Jiang W, Rossmann MG, Kuhn RJ. 2018. Flaviviruses have imperfect icosahedral symmetry. *Proc Natl Acad Sci U S A* 115:11608–11612. <https://doi.org/10.1073/pnas.1809304115>.
5. Tan TY, Fibriansah G, Kostyuchenko VA, Ng TS, Lim XX, Zhang S, Lim XN, Wang J, Shi J, Morais MC, Corti D, Lok SM. 2020. Capsid protein structure in Zika virus reveals the flavivirus assembly process. *Nat Commun* 11: 895. <https://doi.org/10.1038/s41467-020-14647-9>.
6. Lobigs M, Lee E. 2004. Inefficient signalase cleavage promotes efficient nucleocapsid incorporation into budding flavivirus membranes. *J Virol* 78:178–186. <https://doi.org/10.1128/jvi.78.1.178-186.2004>.
7. Lobigs M, Lee E, Ng ML, Pavy M, Lobigs P. 2010. A flavivirus signal peptide balances the catalytic activity of two proteases and thereby facilitates virus morphogenesis. *Virology* 401:80–89. <https://doi.org/10.1016/j.virol.2010.02.008>.
8. Amberg SM, Rice CM. 1999. Mutagenesis of the NS2B-NS3-mediated cleavage site in the flavivirus capsid protein demonstrates a requirement for coordinated processing. *J Virol* 73:8083–8094. <https://doi.org/10.1128/JVI.73.10.8083-8094.1999>.
9. Laureti M, Narayanan D, Rodriguez-Andres J, Fazakerley JK, Kedzierski L. 2018. Flavivirus receptors: diversity, identity, and cell entry. *Front Immunol* 9:2180. <https://doi.org/10.3389/fimmu.2018.02180>.
10. Chu JJ, Ng ML. 2004. Infectious entry of West Nile virus occurs through a clathrin-mediated endocytic pathway. *J Virol* 78:10543–10555. <https://doi.org/10.1128/JVI.78.19.10543-10555.2004>.
11. Glasner DR, Puerta-Guardo H, Beatty PR, Harris E. 2018. The good, the bad, and the shocking: the multiple roles of dengue virus nonstructural protein 1 in protection and pathogenesis. *Annu Rev Virol* 5:227–253. <https://doi.org/10.1146/annurev-virology-101416-041848>.
12. Luo D, Xu T, Hunke C, Gruber G, Vasudevan SG, Lescar J. 2008. Crystal structure of the NS3 protease-helicase from dengue virus. *J Virol* 82: 173–183. <https://doi.org/10.1128/JVI.01788-07>.
13. Issur M, Geiss BJ, Bougie I, Picard-Jean F, Despins S, Mayette J, Hobbey SE, Bisaillon M. 2009. The flavivirus NS5 protein is a true RNA guanylyltransferase that catalyzes a two-step reaction to form the RNA cap structure. *RNA* 15:2340–2350. <https://doi.org/10.1261/rna.1609709>.
14. Steffens S, Thiel HJ, Behrens SE. 1999. The RNA-dependent RNA polymerases of different members of the family *Flaviviridae* exhibit similar properties *in vitro*. *J Gen Virol* 80:2583–2590. <https://doi.org/10.1099/0022-1317-80-10-2583>.
15. Koschinski A, Wengler G, Wengler G, Repp H. 2003. The membrane proteins of flaviviruses form ion-permeable pores in the target membrane after fusion: identification of the pores and analysis of their possible role in virus infection. *J Gen Virol* 84:1711–1721. <https://doi.org/10.1099/vir.0.19062-0>.
16. Kiermayr S, Kofler RM, Mandl CW, Messner P, Heinz FX. 2004. Isolation of capsid protein dimers from the tick-borne encephalitis flavivirus and *in vitro* assembly of capsid-like particles. *J Virol* 78:8078–8084. <https://doi.org/10.1128/JVI.78.15.8078-8084.2004>.
17. Byk LA, Iglesias NG, De Maio FA, Gebhard LG, Rossi M, Gamarnik AV. 2016. Dengue virus genome uncoating requires ubiquitination. *mBio* 7:e00804-16. <https://doi.org/10.1128/mBio.00804-16>.
18. van den Boom J, Meyer H. 2018. VCP/p97-mediated unfolding as a principle in protein homeostasis and signaling. *Mol Cell* 69:182–194. <https://doi.org/10.1016/j.molcel.2017.10.028>.
19. Ye Y, Tang WK, Zhang T, Xia D. 2017. A mighty “protein extractor” of the cell: structure and function of the p97/CDC48 ATPase. *Front Mol Biosci* 4:39. <https://doi.org/10.3389/fmolb.2017.00039>.
20. Davies JM, Brunger AT, Weis WI. 2008. Improved structures of full-length p97, an AAA ATPase: implications for mechanisms of nucleotide-dependent conformational change. *Structure* 16:715–726. <https://doi.org/10.1016/j.str.2008.02.010>.
21. Banerjee S, Bartesaghi A, Merk A, Rao P, Bulfer SL, Yan Y, Green N, Mroczkowski B, Neitz RJ, Wipf P, Falconieri V, Deshaies RJ, Milne JL, Huryn D, Arkin M, Subramaniam S. 2016. 2.3 Å resolution cryo-EM structure of human p97 and mechanism of allosteric inhibition. *Science* 351:871–875. <https://doi.org/10.1126/science.aad7974>.
22. Chapman E, Maksim N, de la Cruz F, La Clair JJ. 2015. Inhibitors of the AAA+ chaperone p97. *Molecules* 20:3027–3049. <https://doi.org/10.3390/molecules20023027>.
23. Lindenbach BD, Rice CM. 1997. *trans*-Complementation of yellow fever virus NS1 reveals a role in early RNA replication. *J Virol* 71:9608–9617. <https://doi.org/10.1128/JVI.71.12.9608-9617.1997>.
24. Stoyanov CT, Boscardin SB, Deroubaix S, Barba-Spaeth G, Franco D, Nussenzweig RS, Nussenzweig M, Rice CM. 2010. Immunogenicity and protective efficacy of a recombinant yellow fever vaccine against the murine malarial parasite *Plasmodium yoelii*. *Vaccine* 28:4644–4652. <https://doi.org/10.1016/j.vaccine.2010.04.071>.
25. Yi Z, Sperzel L, Nurnberger C, Bredenbeek PJ, Lubick KJ, Best SM, Stoyanov CT, Law LM, Yuan Z, Rice CM, MacDonald MR. 2011. Identification and characterization of the host protein DNAJC14 as a broadly active flavivirus replication modulator. *PLoS Pathog* 7:e1001255. <https://doi.org/10.1371/journal.ppat.1001255>.
26. Schoggins JW, Dorner M, Feulner M, Imanaka N, Murphy MY, Ploss A, Rice CM. 2012. Dengue reporter viruses reveal viral dynamics in interferon receptor-deficient mice and sensitivity to interferon effectors *in vitro*. *Proc Natl Acad Sci U S A* 109:14610–14615. <https://doi.org/10.1073/pnas.1212379109>.
27. England CG, Ehlerding EB, Cai W. 2016. NanoLuc: a small luciferase is brightening up the field of bioluminescence. *Bioconjug Chem* 27: 1175–1187. <https://doi.org/10.1021/acs.bioconjugchem.6b00112>.
28. Bredenbeek PJ, Kooi EA, Lindenbach B, Huijckman N, Rice CM, Spaan WJ. 2003. A stable full-length yellow fever virus cDNA clone and the role of conserved RNA elements in flavivirus replication. *J Gen Virol* 84: 1261–1268. <https://doi.org/10.1099/vir.0.18860-0>.
29. Hahn CS, Hahn YS, Rice CM, Lee E, Dalgarno L, Strauss EG, Strauss JH. 1987. Conserved elements in the 3′ untranslated region of flavivirus RNAs and potential cyclization sequences. *J Mol Biol* 198:33–41. [https://doi.org/10.1016/0022-2836\(87\)90455-4](https://doi.org/10.1016/0022-2836(87)90455-4).
30. van der Schaar HM, Rust MJ, Chen C, van der Ende-Metselaar H, Wilschut J, Zhuang X, Smit JM. 2008. Dissecting the cell entry pathway of dengue virus by single-particle tracking in living cells. *PLoS Pathog* 4:e1000244. <https://doi.org/10.1371/journal.ppat.1000244>.
31. Lian W, Jang J, Potosopon S, Li PC, Rahmeh A, Wang J, Kwiatkowski NP, Gray NS, Yang PL. 2018. Discovery of immunologically inspired small molecules that target the viral envelope protein. *ACS Infect Dis* 4:1395–1406. <https://doi.org/10.1021/acscinfecdis.8b00127>.
32. Hackett BA, Cherry S. 2018. Flavivirus internalization is regulated by a size-dependent endocytic pathway. *Proc Natl Acad Sci U S A* 115: 4246–4251. <https://doi.org/10.1073/pnas.1720032115>.
33. Mar KB, Rinkenberger NR, Boys IN, Eitson JL, McDougal MB, Richardson RB, Schoggins JW. 2018. LY6E mediates an evolutionarily conserved enhancement of virus infection by targeting a late entry step. *Nat Commun* 9:3603. <https://doi.org/10.1038/s41467-018-06000-y>.
34. Campos RK, Wong B, Xie X, Lu YF, Shi PY, Pompon J, Garcia-Blanco MA, Bradrick SS. 2017. RPLP1 and RPLP2 are essential flavivirus host factors that promote early viral protein accumulation. *J Virol* 91:e01706-16.
35. Guo F, Wu S, Julander J, Ma J, Zhang X, Kulp J, Cuconati A, Block TM, Du Y, Guo JT, Chang J. 2016. A novel benzodiazepine compound inhibits yellow fever virus infection by specifically targeting NS4B protein. *J Virol* 90:10774–10788. <https://doi.org/10.1128/JVI.01253-16>.
36. Yang Y, Kitagaki J, Dai RM, Tsai YC, Lorick KL, Ludwig RL, Pierre SA, Jensen JP, Davydov IV, Oberoi P, Li CC, Kenten JH, Beutler JA, Voutsden KH, Weissman AM. 2007. Inhibitors of ubiquitin-activating enzyme (E1), a new class of potential cancer therapeutics. *Cancer Res* 67:9472–9481. <https://doi.org/10.1158/0008-5472.CAN-07-0568>.
37. Wojcik C, Yano M, DeMartino GN. 2004. RNA interference of valosin-containing protein (VCP/p97) reveals multiple cellular roles linked to ubiquitin/proteasome-dependent proteolysis. *J Cell Sci* 117:281–292. <https://doi.org/10.1242/jcs.00841>.
38. Chou TF, Brown SJ, Minond D, Nordin BE, Li K, Jones AC, Chase P,

- Porubsky PR, Stoltz BM, Schoenen FJ, Patricelli MP, Hodder P, Rosen H, Deshaies RJ. 2011. Reversible inhibitor of p97, DBeQ, impairs both ubiquitin-dependent and autophagic protein clearance pathways. *Proc Natl Acad Sci U S A* 108:4834–4839. <https://doi.org/10.1073/pnas.1015312108>.
39. Magnaghi P, D'Alessio R, Valsasina B, Avanzi N, Rizzi S, Asa D, Gasparri F, Cozzi L, Cucchi U, Orrenius C, Polucci P, Ballinari D, Perra C, Leone A, Cervi G, Casale E, Xiao Y, Wong C, Anderson DJ, Galvani A, Donati D, O'Brien T, Jackson PK, Isacchi A. 2013. Covalent and allosteric inhibitors of the ATPase VCP/p97 induce cancer cell death. *Nat Chem Biol* 9:548–556. <https://doi.org/10.1038/nchembio.1313>.
40. Weisz OA. 2003. Acidification and protein traffic. *Int Rev Cytol* 226: 259–319. [https://doi.org/10.1016/s0074-7696\(03\)01005-2](https://doi.org/10.1016/s0074-7696(03)01005-2).
41. Gollins SW, Porterfield JS. 1986. The uncoating and infectivity of the flavivirus West Nile on interaction with cells: effects of pH and ammonium chloride. *J Gen Virol* 67:1941–1950. <https://doi.org/10.1099/0022-1317-67-9-1941>.
42. Gollins SW, Porterfield JS. 1985. Flavivirus infection enhancement in macrophages: an electron microscopic study of viral cellular entry. *J Gen Virol* 66:1969–1982. <https://doi.org/10.1099/0022-1317-66-9-1969>.
43. Helenius A. 2018. Virus entry: looking back and moving forward. *J Mol Biol* 430:1853–1862. <https://doi.org/10.1016/j.jmb.2018.03.034>.
44. Klasse PJ. 2015. Molecular determinants of the ratio of inert to infectious virus particles. *Prog Mol Biol Transl Sci* 129:285–326. <https://doi.org/10.1016/bs.pmbts.2014.10.012>.
45. van der Schaar HM, Rust MJ, Waarts BL, van der Ende-Metselaar H, Kuhn RJ, Wilschut J, Zhuang X, Smit JM. 2007. Characterization of the early events in dengue virus cell entry by biochemical assays and single-virus tracking. *J Virol* 81:12019–12028. <https://doi.org/10.1128/JVI.00300-07>.
46. Potokar M, Korva M, Jorgačevski J, Avšič-Županc T, Zorec R. 2014. Tick-borne encephalitis virus infects rat astrocytes but does not affect their viability. *PLoS One* 9:e86219. <https://doi.org/10.1371/journal.pone.0086219>.
47. Pierson TC, Diamond MS. 2012. Degrees of maturity: the complex structure and biology of flaviviruses. *Curr Opin Virol* 2:168–175. <https://doi.org/10.1016/j.coviro.2012.02.011>.
48. Gehrke R, Heinz FX, Davis NL, Mandl CW. 2005. Heterologous gene expression by infectious and replicon vectors derived from tick-borne encephalitis virus and direct comparison of this flavivirus system with an alphavirus replicon. *J Gen Virol* 86:1045–1053. <https://doi.org/10.1099/vir.0.80677-0>.
49. He Y, Liu P, Wang T, Wu Y, Lin X, Wang M, Jia R, Zhu D, Liu M, Zhao X, Yang Q, Wu Y, Zhang S, Liu Y, Zhang L, Yu Y, Pan L, Chen S, Cheng A. 2019. Genetically stable reporter virus, subgenomic replicon and packaging system of duck Tembusu virus based on a reverse genetics system. *Virology* 533:86–92. <https://doi.org/10.1016/j.virol.2019.05.003>.
50. Kassar TC, Magalhães T, S JVV, Carvalho AGO, Silva ANMRDA, Queiroz SRA, Bertani GR, Gil LHV. 2017. Construction and characterization of a recombinant yellow fever virus stably expressing *Gaussia* luciferase. *An Acad Bras Cienc* 89:2119–2130. <https://doi.org/10.1590/0001-3765201720160196>.
51. Pierson TC, Diamond MS, Ahmed AA, Valentine LE, Davis CW, Samuel MA, Hanna SL, Puffer BA, Doms RW. 2005. An infectious West Nile virus that expresses a GFP reporter gene. *Virology* 334:28–40. <https://doi.org/10.1016/j.virol.2005.01.021>.
52. Puig-Basagoiti F, Deas TS, Ren P, Tilgner M, Ferguson DM, Shi PY. 2005. High-throughput assays using a luciferase-expressing replicon, virus-like particles, and full-length virus for West Nile virus drug discovery. *Antimicrob Agents Chemother* 49:4980–4988. <https://doi.org/10.1128/AAC.49.12.4980-4988.2005>.
53. Tamura T, Fukuhara T, Uchida T, Ono C, Mori H, Sato A, Fauzyah Y, Okamoto T, Kurosu T, Setoh YX, Imamura M, Tautz N, Sakoda Y, Khromykh AA, Chayama K, Matsuura Y. 2018. Characterization of recombinant *Flaviviridae* viruses possessing a small reporter tag. *J Virol* 92:e01582-17. <https://doi.org/10.1128/JVI.01582-17>.
54. Zou G, Xu HY, Qing M, Wang QY, Shi PY. 2011. Development and characterization of a stable luciferase dengue virus for high-throughput screening. *Antiviral Res* 91:11–19. <https://doi.org/10.1016/j.antiviral.2011.05.001>.
55. Zhang Q, Li N, Deng C, Zhang Z, Li X, Yoshii K, Ye H, Zhang B. 2019. *trans*-Complementation of replication-defective Omsk hemorrhagic fever virus for antiviral study. *Virol Sin* <https://doi.org/10.1007/s12250-019-00109-0>.
56. Hall MP, Unch J, Binkowski BF, Valley MP, Butler BL, Wood MG, Otto P, Zimmerman K, Vidugiris G, Machleidt T, Robers MB, Benink HA, Eggers CT, Slater MR, Meisenheimer PL, Klaubert DH, Fan F, Encell LP, Wood KV. 2012. Engineered luciferase reporter from a deep sea shrimp utilizing a novel imidazopyrazinone substrate. *ACS Chem Biol* 7:1848–1857. <https://doi.org/10.1021/cb3002478>.
57. Khromykh AA, Sedlak PL, Guyatt KJ, Hall RA, Westaway EG. 1999. Efficient trans-complementation of the flavivirus Kunjin NS5 protein but not of the NS1 protein requires its coexpression with other components of the viral replicase. *J Virol* 73:10272–10280. <https://doi.org/10.1128/JVI.73.12.10272-10280.1999>.
58. Lindenbach BD. 2009. Measuring HCV infectivity produced in cell culture and *in vivo*. *Methods Mol Biol* 510:329–336. https://doi.org/10.1007/978-1-59745-394-3_24.
59. Plaszczyca A, Scaturro P, Neufeldt CJ, Cortese M, Cerikan B, Ferla S, Brancale A, Pichlmair A, Bartenschlager R. 2019. A novel interaction between dengue virus nonstructural protein 1 and the NS4A-2K-4B precursor is required for viral RNA replication but not for formation of the membranous replication organelle. *PLoS Pathog* 15:e1007736. <https://doi.org/10.1371/journal.ppat.1007736>.
60. Youn S, Li T, McCune BT, Edeling MA, Fremont DH, Cristea IM, Diamond MS. 2012. Evidence for a genetic and physical interaction between nonstructural proteins NS1 and NS4B that modulates replication of West Nile virus. *J Virol* 86:7360–7371. <https://doi.org/10.1128/JVI.00157-12>.
61. Akey DL, Brown WC, Dutta S, Konwerski J, Jose J, Jurkiw TJ, DelProposto J, Ogata CM, Skiniotis G, Kuhn RJ, Smith JL. 2014. Flavivirus NS1 structures reveal surfaces for associations with membranes and the immune system. *Science* 343:881–885. <https://doi.org/10.1126/science.1247749>.
62. Lindenbach BD, Rice CM. 1999. Genetic interaction of flavivirus nonstructural proteins NS1 and NS4A as a determinant of replicase function. *J Virol* 73:4611–4621. <https://doi.org/10.1128/JVI.73.6.4611-4621.1999>.
63. Youn S, Ambrose RL, Mackenzie JM, Diamond MS. 2013. Nonstructural protein-1 is required for West Nile virus replication complex formation and viral RNA synthesis. *Virol J* 10:339. <https://doi.org/10.1186/1743-422X-10-339>.
64. Zhang HL, Ye HQ, Deng CL, Liu SQ, Shi PY, Qin CF, Yuan ZM, Zhang B. 2017. Generation and characterization of West Nile pseudo-infectious reporter virus for antiviral screening. *Antiviral Res* 141:38–47. <https://doi.org/10.1016/j.antiviral.2017.02.006>.
65. Acosta EG, Castilla V, Damonte EB. 2009. Alternative infectious entry pathways for dengue virus serotypes into mammalian cells. *Cell Microbiol* 11:1533–1549. <https://doi.org/10.1111/j.1462-5822.2009.01345.x>.
66. Krishnan MN, Sukumaran B, Pal U, Agaisse H, Murray JL, Hodge TW, Fikrig E. 2007. Rab 5 is required for the cellular entry of dengue and West Nile viruses. *J Virol* 81:4881–4885. <https://doi.org/10.1128/JVI.02210-06>.
67. Mosso C, Galvan-Mendoza IJ, Ludert JE, del Angel RM. 2008. Endocytic pathway followed by dengue virus to infect the mosquito cell line C6/36 HT. *Virology* 378:193–199. <https://doi.org/10.1016/j.virol.2008.05.012>.
68. Acosta EG, Castilla V, Damonte EB. 2008. Functional entry of dengue virus into *Aedes albopictus* mosquito cells is dependent on clathrin-mediated endocytosis. *J Gen Virol* 89:474–484. <https://doi.org/10.1099/vir.0.83357-0>.
69. Heinz FX, Auer G, Stiasny K, Holzmann H, Mandl C, Guirakhoo F, Kunz C. 1994. The interactions of the flavivirus envelope proteins: implications for virus entry and release. *Arch Virol Suppl* 9:339–348. https://doi.org/10.1007/978-3-7091-9326-6_34.
70. Krishnan MN, Ng A, Sukumaran B, Gilfoy FD, Uchil PD, Sultana H, Brass AL, Adametz R, Tsui M, Qian F, Montgomery RR, Lev S, Mason PW, Koski RA, Elledge SJ, Xavier RJ, Agaisse H, Fikrig E. 2008. RNA interference screen for human genes associated with West Nile virus infection. *Nature* 455:242–245. <https://doi.org/10.1038/nature07207>.
71. Fernandez-Garcia MD, Meertens L, Bonazzi M, Cossart P, Arenzana-Seisdedos F, Amara A. 2011. Appraising the roles of CBL1 and the ubiquitin/proteasome system for flavivirus entry and replication. *J Virol* 85:2980–2989. <https://doi.org/10.1128/JVI.02483-10>.
72. Wang S, Liu H, Zu X, Liu Y, Chen L, Zhu X, Zhang L, Zhou Z, Xiao G, Wang W. 2016. The ubiquitin-proteasome system is essential for the productive entry of Japanese encephalitis virus. *Virology* 498:116–127. <https://doi.org/10.1016/j.virol.2016.08.013>.
73. Greene W, Zhang W, He M, Witt C, Ye F, Gao SJ. 2012. The ubiquitin/proteasome system mediates entry and endosomal trafficking of Kaposi's sarcoma-associated herpesvirus in endothelial cells. *PLoS Pathog* 8:e1002703. <https://doi.org/10.1371/journal.ppat.1002703>.
74. Park CW, Ryu KY. 2014. Cellular ubiquitin pool dynamics and homeosta-

- sis. *BMB Rep* 47:475–482. <https://doi.org/10.5483/bmbrep.2014.47.9.128>.
75. Xu Q, Farah M, Webster JM, Wojcikiewicz RJ. 2004. Bortezomib rapidly suppresses ubiquitin thiolesterification to ubiquitin-conjugating enzymes and inhibits ubiquitination of histones and type I inositol 1,4,5-trisphosphate receptor. *Mol Cancer Ther* 3:1263–1269.
 76. McDowell GS, Philpott A. 2013. Non-canonical ubiquitylation: mechanisms and consequences. *Int J Biochem Cell Biol* 45:1833–1842. <https://doi.org/10.1016/j.biocel.2013.05.026>.
 77. Li JM, Wu H, Zhang W, Blackburn MR, Jin J. 2014. The p97-UFD1L-NPL4 protein complex mediates cytokine-induced I κ B α proteolysis. *Mol Cell Biol* 34:335–347. <https://doi.org/10.1128/MCB.01190-13>.
 78. Stolz A, Hilt W, Buchberger A, Wolf DH. 2011. Cdc48: a power machine in protein degradation. *Trends Biochem Sci* 36:515–523. <https://doi.org/10.1016/j.tibs.2011.06.001>.
 79. Brandman O, Stewart-Ornstein J, Wong D, Larson A, Williams CC, Li GW, Zhou S, King D, Shen PS, Weibezahn J, Dunn JG, Rouskin S, Inada T, Frost A, Weissman JS. 2012. A ribosome-bound quality control complex triggers degradation of nascent peptides and signals translation stress. *Cell* 151:1042–1054. <https://doi.org/10.1016/j.cell.2012.10.044>.
 80. Verma R, Oania RS, Kolawa NJ, Deshaies RJ. 2013. Cdc48/p97 promotes degradation of aberrant nascent polypeptides bound to the ribosome. *Elife* 2:e00308. <https://doi.org/10.7554/eLife.00308>.
 81. Kloppsteck P, Ewens CA, Forster A, Zhang X, Freemont PS. 2012. Regulation of p97 in the ubiquitin-proteasome system by the UBX protein-family. *Biochim Biophys Acta* 1823:125–129. <https://doi.org/10.1016/j.bbamcr.2011.09.006>.
 82. Hanzelmann P, Schindelin H. 2017. The interplay of cofactor interactions and posttranslational modifications in the regulation of the AAA+ ATPase p97. *Front Mol Biosci* 4:21. <https://doi.org/10.3389/fmolb.2017.00021>.
 83. Phongphaew W, Kobayashi S, Sasaki M, Carr M, Hall WW, Orba Y, Sawa H. 2017. Valosin-containing protein (VCP/p97) plays a role in the replication of West Nile virus. *Virus Res* 228:114–123. <https://doi.org/10.1016/j.virusres.2016.11.029>.
 84. Wong HH, Kumar P, Tay FP, Moreau D, Liu DX, Bard F. 2015. Genome-wide screen reveals valosin-containing protein requirement for coronavirus exit from endosomes. *J Virol* 89:11116–11128. <https://doi.org/10.1128/JVI.01360-15>.
 85. Panda D, Rose PP, Hanna SL, Gold B, Hopkins KC, Lyde RB, Marks MS, Cherry S. 2013. Genome-wide RNAi screen identifies SEC61A and VCP as conserved regulators of Sindbis virus entry. *Cell Rep* 5:1737–1748. <https://doi.org/10.1016/j.celrep.2013.11.028>.
 86. Carissimo G, Chan YH, Utt A, Chua TK, Bakar FA, Merits A, Ng L. 2019. VCP/p97 is a proviral host factor for replication of chikungunya virus and other alphaviruses. *Front Microbiol* 10:2236. <https://doi.org/10.3389/fmicb.2019.02236>.
 87. Yi Z, Fang C, Zou J, Xu J, Song W, Du X, Pan T, Lu H, Yuan Z. 2016. Affinity purification of the hepatitis C virus replicase identifies valosin-containing protein, a member of the ATPases associated with diverse cellular activities family, as an active virus replication modulator. *J Virol* 90:9953–9966. <https://doi.org/10.1128/JVI.01140-16>.
 88. Yi Z, Yuan Z. 2017. Aggregation of a hepatitis C virus replicase module induced by ablation of p97/VCP. *J Gen Virol* 98:1667–1678. <https://doi.org/10.1099/jgv.0.000828>.
 89. Ernst R, Mueller B, Ploegh HL, Schlieker C. 2009. The otubain YOD1 is a deubiquitinating enzyme that associates with p97 to facilitate protein dislocation from the ER. *Mol Cell* 36:28–38. <https://doi.org/10.1016/j.molcel.2009.09.016>.
 90. Onorati M, Li Z, Liu F, Sousa AMM, Nakagawa N, Li M, Dell'Anno MT, Gulden FO, Pochareddy S, Tebbenkamp ATN, Han W, Pletikos M, Gao T, Zhu Y, Bichsel C, Varela L, Szigeti-Buck K, Lisgo S, Zhang Y, Testen A, Gao X-B, Mlakar J, Popovic M, Flamand M, Strittmatter SM, Kaczmarek LK, Anton ES, Horvath TL, Lindenbach BD, Sestan N. 2016. Zika virus disrupts phospho-TBK1 localization and mitosis in human neuroepithelial stem cells and radial glia. *Cell Rep* 16:2576–2592. <https://doi.org/10.1016/j.celrep.2016.08.038>.
 91. Lin JD, Feng N, Sen A, Balan M, Tseng HC, McElrath C, Smirnov SV, Peng J, Yasukawa LL, Durbin RK, Durbin JE, Greenberg HB, Kotenko SV. 2016. Distinct roles of type I and type III interferons in intestinal immunity to homologous and heterologous rotavirus infections. *PLoS Pathog* 12:e1005600. <https://doi.org/10.1371/journal.ppat.1005600>.